Role of guest-host intermolecular forces in photoinduced reorientation of dyed liquid crystals

L. Marrucci, D. Paparo, P. Maddalena, E. Massera, E. Prudnikova,[a] and E. Santamato
INFM and Dipartimento di Scienze Fisiche, Università ''Federico II'', Mostra d'Oltremare Pad. 20, 80125 Napoli, Italy

(Received 4 June 1997; accepted 11 September 1997)

An experimental study of the photoinduced molecular reorientation of dyed liquid crystals for a set of guest-host combinations is reported. We find large variations in the magnitude of the effect for different dyes but also for different hosts, with polar hosts resulting often significantly more effective than nonpolar ones. The data are interpreted in terms of a kinetic mean-field model for the dye molecule rotational dynamics and interaction with the liquid crystal host. The results point to a significant variation of guest-host intermolecular forces upon photoinduced electronic excitation of dye molecules. This force variation is reflected in a variation of dye molecule physical parameters such as the rotational friction coefficient and the orientational mean-field energy. © *1997 American Institute of Physics.* [S0021-9606(97)51647-3]

I. INTRODUCTION

A laser beam passing through a transparent nematic liquid crystals (LC) is able to induce a large change in the average molecular orientation.[1,2] This phenomenon is well understood as the effect of the optical torque acting on the molecules due to their anisotropic optical polarizability.[3] Not so clear is the case of light-absorbing LCs. A few years ago, I. Jánossy *et al.* discovered that a small amount of dye dissolved in a LC may lead to a large variation of the optical torque, with almost no change in the material polarizability.[4] A dye weight fraction of less than 0.1% can enhance the optical torque by almost two orders of magnitude and, in some cases, can even change its sign. Presumably, some mechanism related to light absorption comes into play, generating an additional photoinduced torque much larger than the polarization torque. Since its discovery, the phenomenology of the ''dye effect'' has been investigated in detail.[5–14] Heating effects have been excluded from the number of possible mechanisms, as different dyes yield totally different torques even for equal values of light absorbance. Moreover, the reversibility and reproducibility of the effect excludes the occurrence of photochemical irreversible transformations. Nevertheless, the phenomenon is fairly general as it can be observed in almost all LC-dye mixtures. Its generality is even wider than the LC field, as closely related effects have been recently discovered in isotropic liquids,[15,16] and in absorbing Langmuir films.[17]

A molecular model was proposed by I. Jánossy to explain the effect.[18] The model is based on two hypotheses: First, light absorption generates an anisotropic population of electronically excited dye molecules and a corresponding hole in the ground-state dye population; second, excited- and ground-state dye molecules have different intermolecular orientational interactions with the LC host. As a consequence of these two effects, light generates an anisotropic ''molecular mean-field'' acting on the LC host, that produces the additional torque. This model is successful into predicting the main features and order of magnitude of the observed phenomena. However, it still escapes a more quantitative comparison with experiments because it relies upon scarcely known molecular quantities, such as the orientational interaction energy of an excited dye molecule with the host and the dye rotational diffusion constant.

Moreover, even if Jánossy's model is accepted, several important questions remain open. What intermolecular interactions are actually responsible for the effect? What transformation occurs in the excited dye molecule such that intermolecular interactions are significantly altered? What features in the dye (and host) molecule structures mark the difference between a very effective dye and one which does not work, or between a dye providing a positive torque (with respect to the direction of the polarization torque) and a negative one? What determines the observed wavelength dependence of the photoinduced torque?[9,12] What is the origin of the peculiar nonmonotone temperature behavior of the effect reported in Ref. 6?

The model in Ref. 18 is made a little obscure by an incorrect analysis of angular momentum conservation, leading to an expression for the photoinduced torque that is also slightly incorrect. These points have been corrected in Ref. 19, where the model is reanalyzed with a more formal approach. Moreover, in Ref. 18 the force change occurring in a excited dye molecule is modeled only as a change of the orientational mean-field potentials, controlling the equilibrium orientational distribution. In Ref. 19, a variation of nonequilibrium parameters such as the rotational friction coefficient is also allowed. Which parameter change is actually the more important is another open question, and its answer could be essential for a quantitative understanding of experiments.

In this work we report the measurement of the photoinduced reorientation in a set of dye-LC mixtures using a

[a]Present address: Liq. Cryst. Soc. ''Sodruzhestvo,'' 11 Staropetrovsky proezd, Moscow Russia 125130.

pump and probe interferometric technique. The measured magnitude of the effect is given in terms of a merit figure defined in order to highlight the guest-host molecular effects, in the comparison of different mixtures and wavelengths. The merit figure definition and the theory relating it to the experiment are in Sec. II. In Sec. III and IV, our experimental results are presented and discussed in view of other works dealing with dyes and intermolecular interactions in excited states. A more quantitative analysis based on the molecular model of Ref. 19 is finally attempted in Sec. V.

II. THEORETICAL BACKGROUND

The optical reorientation of nematic LCs is driven by the optical torque acting on the molecular director $\boldsymbol{n}$.[3] In transparent LCs, this torque is due to the molecule optical polarization, and it is given by $\boldsymbol{\tau}_o=\epsilon_a/16\pi(\boldsymbol{n}\cdot\boldsymbol{E}^*)(\boldsymbol{n}\times\boldsymbol{E})+c.c.$. In this expression $\boldsymbol{E}$ is the complex amplitude of the optical electric field and $\epsilon_a=\mathrm{Re}(\epsilon_e-\epsilon_o)$, where ϵ_e and ϵ_o are the dielectric constants for $\boldsymbol{E}$ respectively parallel (extraordinary wave) and perpendicular (ordinary wave) to $\boldsymbol{n}$. The dielectric tensor is $\epsilon_{ij}=\epsilon_o\delta_{ij}+(\epsilon_e-\epsilon_o)n_in_j$. In absorbing LCs, the constants ϵ_o and ϵ_e are complex. It is convenient to define also the ordinary and extraordinary refractive indices $n_o=\mathrm{Re}(\sqrt{\epsilon_o})$ and $n_e=\mathrm{Re}(\sqrt{\epsilon_e})$, and absorption coefficients $\alpha_o=(2\pi/n_o\lambda)\mathrm{Im}(\epsilon_o)$ and $\alpha_e=(2\pi/n_e\lambda)\mathrm{Im}(\epsilon_e)$, respectively, where λ is light wavelength in vacuum.

When the LC absorbs light, an additional photoinduced torque $\boldsymbol{\tau}_{\mathrm{ph}}$ is observed, superimposed to $\boldsymbol{\tau}_o$. Provided that the material response is local, symmetry considerations can be used to prove that the photoinduced torque must be given by

$$\boldsymbol{\tau}_{\mathrm{ph}}=\eta\boldsymbol{\tau}_o=\frac{\zeta}{16\pi}(\boldsymbol{n}\cdot\boldsymbol{E}^*)(\boldsymbol{n}\times\boldsymbol{E})+c.c., \tag{1}$$

in the limit of small light intensity. In other words, the photoinduced torque $\boldsymbol{\tau}_{\mathrm{ph}}$ has the same angular dependence on $\boldsymbol{n}$ and $\boldsymbol{E}$ as the polarization optical torque $\boldsymbol{\tau}_o$, but its magnitude is controlled by a new dimensionless material constant $\zeta=\eta\epsilon_a$. Several experiments confirmed Eq. (1). Moreover, they have shown that ζ is proportional to dye concentration, if not too large, and it depends on the dye and host specific molecular structures, on light wavelength, and on temperature. In some guest-host mixtures the torque ratio $\eta=\zeta/\epsilon_a$ may reach values of about 400 for a dye concentration below 1% in weight. Moreover, ζ can also be negative, contrary to ϵ_a that is always positive at optical frequencies. A negative ζ implies that the torque tends to orient $\boldsymbol{n}$ perpendicular to the optical field $\boldsymbol{E}$, instead of parallel.

The photoinduced response of a given dye-LC mixture is completely characterized by its material constant ζ (or enhancement ratio η). The ratio ζ/N_d, where N_d is the dye number-density, characterizes the overall efficiency of a single dye molecule in a given host. However, the parameter ζ/N_d depends trivially on the light absorption efficiency of the dye molecule, i.e., on its absorption cross section σ. Indeed, the very general assumption that the photon absorption events are statistically independent implies that the dye efficiency is proportional to the number of absorbed photons per unit time, provided that all other properties are fixed. Since we are interested mainly in comparing the contribution of the ''other properties,'' it is convenient to drop the dependence on the cross section σ. Since $\sigma N_d\propto(n_e\alpha_e+2n_o\alpha_o)\lambda$ (see Sec. V for a derivation), we introduce the dimensionless merit figure

$$\mu=\frac{\zeta}{(n_e\alpha_e+2n_o\alpha_o)\lambda S}=\frac{\eta}{(n_e\alpha_e+2n_o\alpha_o)\lambda}\frac{\epsilon_a}{S}, \tag{2}$$

where S is the host orientational order parameter. μ retains only the ''interesting'' dependencies of ζ/N_d, but it is independent of the molecular cross section σ for light absorption. Division by S is included for two reasons: First, if S is small we expect $\zeta\propto S$, and therefore μ will be independent of the order parameter S; second, our definition of μ can be extended even to the isotropic phase by considering the enhancement η of the optical Kerr effect and replacing the ratio ϵ_a/S with its isotropic constant limit.[15] This allows us to compare isotropic and nematic phases.

The merit figure μ gives an estimate of the angular momentum imparted to LC molecules per absorbed photon, in units of Planck constant h. Indeed, the angular momentum transferred per unit time and volume to LC molecules is given by the dye-induced torque $\tau_{\mathrm{ph}}\sim\zeta|E|^2/16\pi$. The number of photons absorbed per unit time and volume is given by $N_f=\mathrm{Im}(\epsilon_{ij}E_iE_j^*)/4h\sim\mathrm{Im}(\Sigma_i\epsilon_{ii})|E|^2/12h=\lambda(n_e\alpha_e+2n_o\alpha_o)|E|^2/24\pi h$. The merit figure is then obtained as $\mu\sim\tau_{\mathrm{ph}}/(N_fSh)$, that justifies the above interpretation.

To obtain ζ and μ we measured the nonlinear optical phase shift $\Delta\phi$ induced in a probe beam by effect of the molecular reorientation due to the optical torque exerted by a pump laser beam. Consider a LC film of thickness L sandwiched between two glass walls treated for strong planar alignment, i.e., $\boldsymbol{n}$ parallel to the walls. We choose a coordinate system with the z axis along $\boldsymbol{n}$, and x along the film normal. Let xz be also the common incidence plane of pump and probe beams, both p-polarized.

The x component of the complex wave vector $\boldsymbol{k}$ of a p-polarized plane wave impinging at incidence angle β is

$$k_x=\frac{2\pi}{\lambda}\frac{1}{\epsilon_{xx}}(-\epsilon_{xz}\sin\beta+\sqrt{\epsilon_o\epsilon_e(\epsilon_{xx}-\sin^2\beta)}). \tag{3}$$

Since ϵ_{ij} is complex, k_x is complex as well. Its real part defines the optical phase change along the x axis, and its imaginary part the amplitude decay due to absorption. In the undistorted planar sample, $\epsilon_{xx}=\epsilon_o,\epsilon_{zz}=\epsilon_e,\epsilon_{xz}=0$. The absorption coefficient is then

$$\alpha_x=2\mathrm{Im}(k_x)=\frac{n_o\alpha_e-\frac{n_e}{n_o}\left(\frac{\alpha_e}{n_e}-\frac{\alpha_o}{n_o}\right)\sin^2\beta}{\sqrt{n_o^2-\sin^2\beta}}. \tag{4}$$

The x-component of the Poynting vector inside the sample is

$$S_x(x)=T_0I_0\cos\beta\ e^{-\alpha_xx}, \tag{5}$$

where T_0 is the transmission coefficient at the input face and I_0 is the intensity of the beam entering the sample. The total (dye + polarization) optical torque due to the pump is therefore given by

$$\tau_y(x) = \frac{(\zeta+\epsilon_a)}{n_o^2 c} S_x(x) \sin\beta_0 = \frac{(\zeta+\epsilon_a)}{2n_o^2 c} \sin(2\beta_0) T_0 I_0 e^{-\alpha_x x}, \quad (6)$$

and $\tau_x = \tau_z = 0$, where β_0 is the pump beam incidence angle, and α_x is given by Eq. (4) with $\beta = \beta_0$.

The balance between the total optical torque and the elastic torque determines the steady-state reorientation angle $\gamma(x)$ of $\boldsymbol{n}$ off the z axis, in the xz plane. In a linearized approximation for small light intensity and small $\gamma(x)$, we have

$$K_{11}\frac{d^2\gamma}{dx^2} = -\tau_y(x), \quad (7)$$

where K_{11} is the splay elastic constant. The boundary conditions are $\gamma(0) = \gamma(L) = 0$. The solution to Eq. (7) is

$$\gamma(x) = \frac{\tau_y(0)}{K_{11}\alpha_x^2}\left[(1-e^{-\alpha_x x}) - \frac{x}{L}(1-e^{-\alpha_x L})\right], \quad (8)$$

with $\tau_y(0)$ given by Eq. (6) for $x = 0$.

The small director reorientation will correspond to a change

$$\delta k_x(x) = \frac{2\pi(\epsilon_e - \epsilon_o)}{\lambda n_o^2} \sin\beta_1 \quad \gamma(x), \quad (9)$$

in the probe wave vector, where β_1 is the probe incidence angle. The probe optical phase shift at the sample output is then

$$\Delta\phi = \mathrm{Re}\left(\int_0^L \delta k_x \quad dx\right) = (\zeta+\epsilon_a)\frac{\pi\epsilon_a L^3 f T_0 \sin 2\beta_0 \sin\beta_1}{12\lambda c n_o^4 K_{11}} I_0, \quad (10)$$

where the effect of absorption losses is included in the factor

$$f = \frac{12}{(\alpha_x L)^2}\left[1 - \left(\frac{1}{2} + \frac{1}{\alpha_x L}\right)(1-e^{-\alpha_x L})\right], \quad (11)$$

($f = 1$ for a transparent sample). Eq. (10) is a plane-wave expression. In the finite Gaussian beam case, the same expression can be still used as a reasonable approximation for the phase shift induced in the pump-beam spot center by using the effective intensity $I_0 = 2P_0/g\pi w_0^2$, where P_0 is the pump beam power, w_0 is its $1/e^2$-radius, and $g(w_0/L)$ is a factor taking into account the transverse elastic effects ($g = 1$ in the plane wave limit).[20] In our case $w_0/L = 0.8$, corresponding to $g \simeq 4$.

III. EXPERIMENT

The nonlinear optical phase shift $\Delta\phi$ was measured by means of an interferometric technique, similar to that described in Ref. 21. The sample was placed in a arm of a Mach–Zender interferometer based on a He–Ne laser. The beam passing through the sample acted as probe and was not focused. The two beams of the interferometer were recombined with a small relative angle, in order to obtain, for a homogeneous sample, an interference pattern of straight parallel fringes on a screen placed at the output of the interferometer. A lens system at the interferometer output produced a magnified image of the sample on the screen, so that the interference actually occurred in ''near field.'' The nonlinear phase-shift transverse profile was measured from the fringe shape deformation. As pump beam, we used the output of a He–Ne laser, an Ar^+ laser, or a dye laser, depending on the wavelength and power needed. The pump was focused to a spot size $w_0 = 40\mu$m. Pump and probe incidence angles were $\beta_0 = 37°$ and $\beta_1 = 43°$, respectively. To erase the additional phase retardation due to thermal indexing, all measurements were performed after blocking the pump beam and waiting the time necessary for complete thermal relaxation, that occurs much faster than the director relaxation time. The systematic error involved in such procedure was estimated to be below 5%. The nonlinear phase shift of pure LC transparent samples was also measured and used as reference.

All LC samples were 50μm thick. The planar alignment was obtained with rubbed polyvinyl alcohol. In separate experiments, we studied a number of mixtures with various dyes, mainly anthraquinone and azo derivatives, and several LC hosts.[22] In this large set, we selected a subset of 9 ''representative'' mixtures, on which we concentrated our analysis. The mixtures of this subset were obtained as combinations of 3 dyes and 3 LC hosts, with a weight–weight ratio of the order of 0.1%. The dye molecular structures are reported in Fig. 1(b). In the same figure it is shown also the molecular axis ξ that is aligned preferentially along the LC director $\boldsymbol{n}$. The dye 1,8-dihydroxy 4,5-diamino, 2,7-diisopentylanthraquinone, here denoted as AD1 (anthraquinone derivative 1), was chosen because it is the most effective positive-ζ dye discovered so far; the dye denoted as AD2 is another positive-ζ dye with a dichroism similar to AD1, but a much smaller ζ; the dye N,N'-(4-methylphenyl)-1,4-diaminoanthraquinone, denoted as AD3, is an effective negative-ζ dye.

The two pure LC host molecules used in our experiments are reported in Fig. 1(a). They are the pentylcyanobiphenyl (5CB) and the *p*-methoxybenzylidene-*p*-*n*-butylinaniline (MBBA). We also used a mixture of cyanophenyls produced by Merck and denoted as E63 (see Ref. 25 for a complete list of its components). The physical properties at the working temperature $T = 24°$C of these three LCs are listed in Table I. The clearing temperature $T_c = 39°$ of our MBBA samples is lower than the known value, due to a small degree of water contamination. The choice of these three hosts was motivated by the following considerations. 5CB has a strong polar head, namely the cyano group

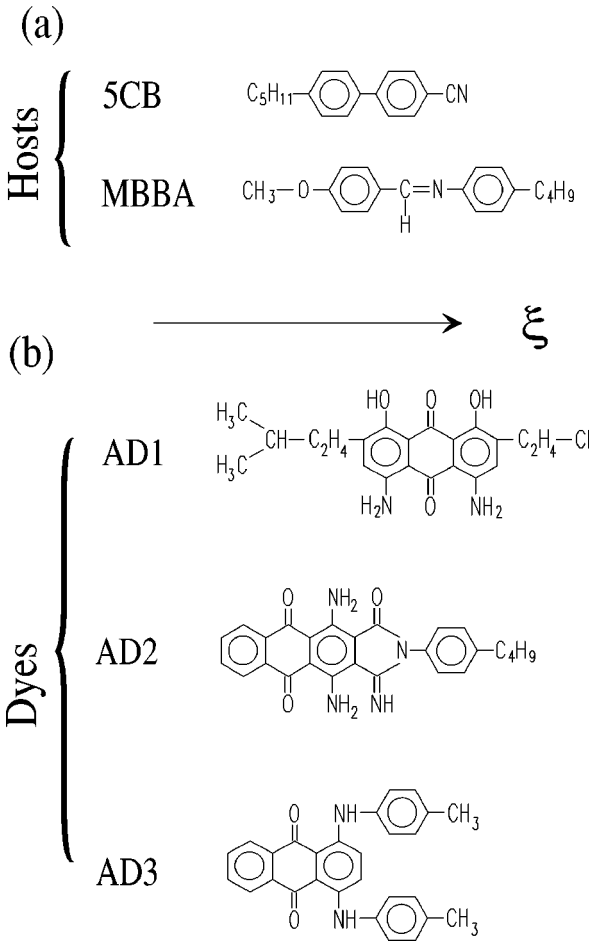

FIG. 1. Structure formulae of employed materials: (a) Hosts; (b) dyes. The molecular axis ξ that is preferentially aligned along the LC molecular director is also reported.

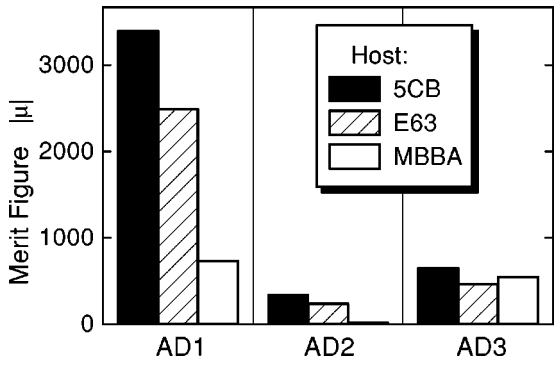

FIG. 2. Bar plot of the measured merit figures (absolute value) $|\mu|$ for 9 guest-host combinations, at temperature $T=24°C$ and wavelength $\lambda=633$ nm. For the AD2-MBBA mixture, μ was below the experimental sensitivity, and the bar indicates its estimated upper bound.

CN, capable of dipole–dipole interactions or even of hydrogen bonding with other polar groups present in the dyes, such as hydroxyl OH, carbonyl CO, or amino NH_2. MBBA has no strong polar groups. E63 is like 5CB as far as polar interactions are concerned. On the other hand, at working temperature, MBBA has a slightly larger birefringence $n_e - n_o$ than 5CB and approximately the same as E63. Roughly speaking, the same relations should hold for the anisotropy of polarizability, and therefore for the anisotropic part of dispersive interactions. By comparing the merit figures of the same dye in 5CB and MBBA, therefore, we should be able to determine if polar interactions are more or less important than dispersive and steric interactions in determining the dye effect. E63 is included mainly for two reasons. First, it is the host that was employed in many of the previous works on the subject and therefore it can be used for comparison. Second, it has a much larger order parameter at working temperature than 5CB and MBBA, and therefore it allows us to investigate the effect of a higher dye order.

The measured properties of the 9 guest-host combinations are reported in Table II. The measured merit figure μ is also shown graphically in Fig. 2. In these measurements, the pump wavelength was $\lambda=633$ nm. It is evident that the polar hosts E63 and 5CB enhance the dye-induced torque effect for the two positive-ζ dyes AD1 and AD2. The AD1-5CB and AD1-E63 mixtures are 4.6 and 3.4 times, respectively, more efficient than the AD1-MBBA one. The reorientation effect was significant in the AD2-5CB and AD2-E63 cases, while it was not even detectable in the AD2-MBBA mixture. On the contrary, the negative-ζ dye AD3 turned out to have approximately the same merit figure in all hosts.

The first conclusion we draw from these data is that specific guest-host intermolecular forces play a major role in the phenomenon. This supports the validity of Jánossy's picture. The data also indicate that dipole–dipole interactions

TABLE I. Properties of host nematic LC materials (for $T=24$ °C). T_c is the clearing temperature (measured in our samples), S the order parameter, K_{11} the splay elastic constant, n_o, n_e the ordinary and extraordinary refractive indices at wavelength $\lambda=633$ nm, respectively.

LC	T_c (°C)	S	K_{11} (10^{-6} dyn)	n_o	n_e	n_e-n_o
5CB	34	0.6[a]	0.55[a]	1.53[b]	1.71[b]	0.18
E63	82	0.75[c]	0.9[d]	1.52[e]	1.74[e]	0.22
MBBA	39	0.6[f]	0.55[f]	1.54[f]	1.76[f]	0.22

[a]N. V. Madhusudana and R. Pratibha, Mol. Cryst. Liq. Cryst. **89**, 249 (1982).
[b]P. P. Karat and N. V. Madhusudana, Mol. Cryst. Liq. Cryst. **36**, 51 (1976).
[c]Reference 25.
[d]I. Jánossy, (private communication).
[e]Merck data sheets.
[f]I. Haller, J. Chem. Phys. **57**, 1400 (1972), and references therein.

TABLE II. Measured properties of dye-LC mixtures for pump and probe wavelength $\lambda = 633$ nm and temperature $T = 24$ °C.

Dye-LC	α_o (cm^{-1})	α_e (cm^{-1})	S_g	u_g (kJ/mol)	$\Delta\phi/P_0$ (rad/mW)	ζ	μ
AD1-5CB	42	190	0.58	35	6.6	58	3400
AD1-E63	68	700	0.82	59	5.7	170	2500
AD1-MBBA	94	190	0.31	16	2.5	18	740
AD2-5CB	82	370	0.58	35	0.92	11	340
AD2-E63	50	480	0.78	49	0.59	11	240
AD2-MBBA	82	350	0.55	30	< 0.2	< 1	< 40
AD3-5CB	98	210	0.32	18	-1.6	-16	-650
AD3-E63	117	360	0.47	21	-1.3	-22	-470
AD3-MBBA	17	38	0.33	17	-0.36	-2.6	-550

seem to contribute to the torque effect significantly more than dispersive and steric interactions for dyes providing positive-ζ torques. When we say dipole–dipole interactions, however, we do not refer to the total dipole of dye and LC molecules (AD1 has no dipole moment in the ξ direction, by symmetry), but rather to the dipole groups (CN, OH, NH_2, CO) present in dye and LC molecules, which can interact rather strongly when they are close to each other. Typical interaction energies are of 5–10 kJ/mol, for each dipole pair.[26] When hydrogen bonding is present, this energy can raise to 20-30 kJ/mol. Hydrogen bonding could take place, for example, between the CN group of 5CB and the OH or NH_2 groups in AD1 and AD2.

That dipole–dipole forces play an important role in the orientational order of dye-LC mixtures is confirmed by the results of Ref. 27, where the dye ground-state order parameter S_g is measured for a large set of dyes in three different hosts, two of which are nonpolar and one has a CN polar group. It was found that S_g changes from 0.3 to 0.8 when plotted versus the length-to-width ratio of dye molecules in the two nonpolar hosts (see Figs. 3 and 4 of Ref. 27), while it is approximately constant to a value between 0.6 and 0.8 in the polar host (Fig. 2 of Ref. 27). Therefore, van der Waals interactions (steric and dispersive) appear to dominate the dye alignment in the nonpolar hosts, while dipole–dipole contributions become also very important in the polar host (the HOMO–LUMO argument used in Ref. 27 to explain such results is, in our opinion, less convincing). Our measurements of the dye order parameter S_g (based on the measured dichroism) confirmed this effect in the case of AD1, as its order parameter in MBBA is much smaller than in 5CB and E63. In Table II we reported also the value of the mean-field orientational energy u_g of dyes in all mixtures, calculated as described in Sec. V.

In synthesis, polar intermolecular forces play a dominant role in the photoinduced torque effect (for positive ζ), and the same forces concur to determine the ground-state dye alignment in the nematic LC host. The negative-ζ dye does not show a similar sensitivity to the specific guest-host interactions, suggesting that other molecular forces could be involved.

We now move to discussing Jánossy's assumption that intermolecular guest-host forces are significantly modified by dye electronic excitation. Although this assumption is always true to some extent,[28] we need to have a quantitative idea of the actual modification occurring in our case, in order to verify the validity of Janossy's model. Let us concentrate on the dye AD1 which, being the most effective one, should be also the easier to understand. The visible absorption spectrum of AD1 in 5CB is reported in Fig. 3(a). To understand such spectrum, we refer to Refs. 29–31 dealing with molecules similar to AD1 in their electronic structure. The qualitative results reported in those works should apply to AD1 as

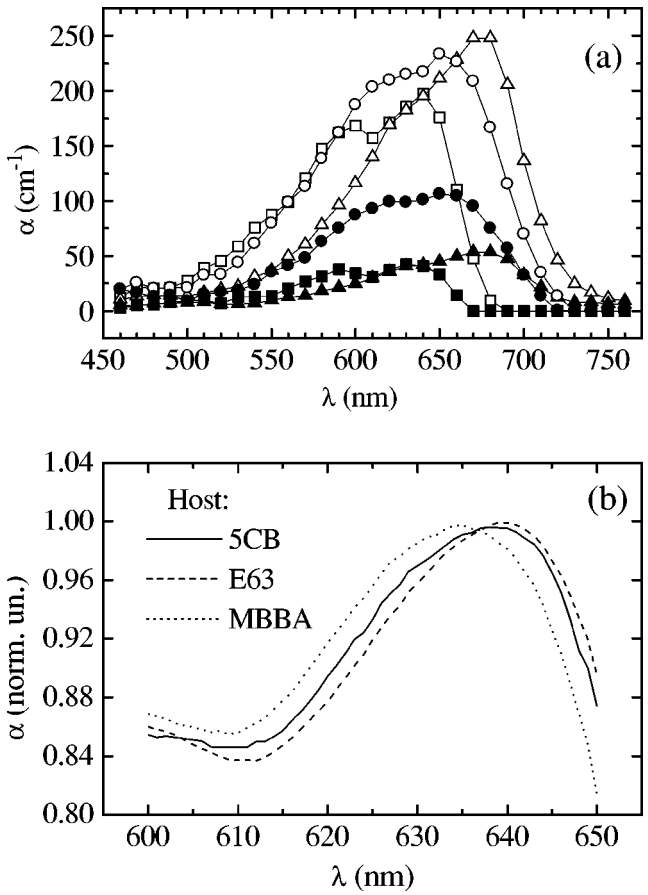

FIG. 3. Absorption spectra of mixtures: (a) parallel (α_e, open symbols) and perpendicular (α_o, filled symbols) absorption coefficients of mixtures of AD1 (squares), AD2 (triangles), and AD3 (circles) in 5CB; (b) detail of absorption peak of AD1 in 5CB, E63, and MBBA, showing the solvent-induced shift (room temperature).

well. The main absorption peak, at a wavelength of about 635–640 nm, can be assigned to a $S_0 \rightarrow S_1$ electronic transition, which is the only electric-dipole-allowed transition in the visible range. The secondary peak, blue-shifted by an amount of about 50 nm, can be assigned to a vibronic excitation between the same electronic levels, as the shift corresponds to the stretch frequency of the bonds between the anthraquinone and the NH_2 and OH substituent groups. The S_0-S_1 transition dipole is parallel to the long molecular axis ξ, thus yielding positive dichroism. The $S_1 \rightarrow S_0$ transition observed in the fluorescence spectrum of AD1 in E63 is peaked at about 660 nm.[32]

In Refs. 29 and 30, the electronic structure of some anthraquinone derivatives is studied theoretically. It is shown that the S_0-S_1 transition is composed by more than 90% of a π-π^* HOMO–LUMO electronic transition, where HOMO is a π orbital having its electron charge density mainly localized on the substituent atoms, i.e., specifically the nitrogen of NH_2 and the oxygen of OH, and LUMO is a π orbital of the unsubstituted anthraquinone, having electronic charge distributed in the whole molecule body including the carbonyl groups. Therefore electronic excitation in AD1 involves a significant intramolecular electron charge transfer from the NH_2 and OH groups to the anthraquinone body. A reduction of electron charge on the NH_2 or OH groups is expected to increase their acidity in the Lewis sense, i.e., their tendency to donate the H^+ proton in a hydrogen bond, or possibly even in a proton-transfer process. A strong enhancement of intermolecular dipole–dipole or hydrogen–bond interactions for the excited AD1 is therefore plausible. We refer to Refs. 33–37 for theoretical and experimental studies of hydrogen–bond strength increase or decrease in consequence of electronic excitation. From the results of these works, we estimate the possible change in interaction energy to be in the range 1–10 kJ/mol, for each polar group.

A direct experimental indication of this effect is provided by the solvent-induced shifts in the absorption spectra. Figure 3(b) reports our measurements of the absorption peak of AD1 dissolved in the three LC hosts. A red-shift of about 5 nm in the polar 5CB and E63 hosts with respect to the nonpolar MBBA is evident. This shift points to hydrogen–bond or dipole–dipole interactions between AD1 and the polar solvents. Moreover, since the shift is toward the red, the interaction in the excited state must be stronger than in the ground state. A shift of 5 nm corresponds approximately to an energy difference of 1.5 kJ/mol. This figure is a lower bound for the complete intermolecular-force energy difference ΔE between excited-state and ground-state dye molecules achieved after complete relaxation of the solvation shell around the excited dye molecule. The solvent-induced shift is even larger in the vibronic band, consistent with the hypothesis that such shift is due to the interaction of the polar substituent groups with the solvent. For $\lambda \sim 550$ nm, the MBBA-5CB shift is of about 8 nm and the MBBA-E63 one is about 16 nm.

Another possibility worth mentioning is that the acidity increase in the NH_2 and OH groups after excitation could lead to an intramolecular proton-transfer process, as proposed for instance in Ref. 23 (see also Ref. 38 for a theoretical study of intramolecular proton-transfer processes). Indeed, when the molecule is in its ground state, a proton of each substituent group is likely to be engaged in intramolecular hydrogen bond with the oxygen of the closest carbonyl group CO of the anthraquinone. After excitation, the proton could be ''donated'' to the carbonyl group, thus swapping covalent and hydrogen bonds. This process would lead to a shift in the equilibrium position of the proton and therefore to a significant change of electrostatic intermolecular interactions. However, this process is probably absent or very unfrequent in AD1-LC mixtures, since no sign of its occurrence is observed in the fluorescence spectrum.[32]

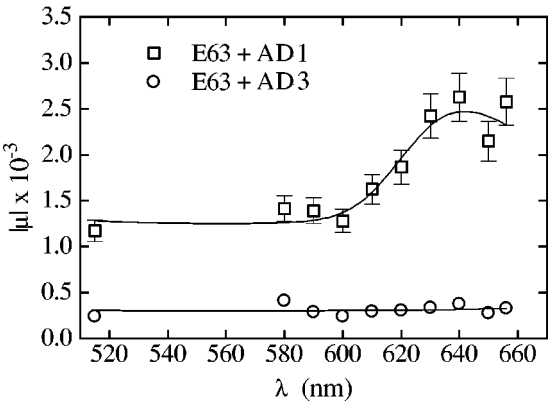

FIG. 4. Experimental and theoretical merit figure μ vs light wavelength λ for AD1 and AD3 in E63 at temperature $T=24°C$.

Besides polar interactions, dispersive and steric forces can also undergo significant variations in consequence of electronic excitation. Reference 39 reports of changes of the molecule polarizability ranging from 10% to 100% for a number of molecules. Such changes can lead to comparable variations of dispersive forces. Steric interactions are obviously changed when photoinduced conformational transformations take place. This is known to occur for example in azo-dyes, but not in most anthraquinone derivatives. However, a conformation change could perhaps take place in AD3, since the two rigid side-groups $NH-C_6H_6-CH_3$ might be reoriented in the excited molecule. This would explain its insensitivity to the host. On the contrary, the high sensitivity to the host polarity seems to exclude an important role of dispersive and conformational effects in the case of AD1 and AD2.

IV. WAVELENGTH DEPENDENCE

The dependence of the photoinduced torque from the pump light wavelength for the mixtures AD1-E63 and AD3-E63 has been already reported in Ref. 9. From those data, we calculated the corresponding dependence of the merit figure μ versus light wavelength, as shown in Fig. 4.

In AD3-E63, the merit figure is found approximately independent of wavelength, as expected. On the contrary, in AD1-E63 a more complex wavelength dependence is observed, that we correlated with the double-band absorption spectrum shown in Fig. 3(a). We made the hypothesis that

each absorption band has its own merit figure, independent of wavelength. Let us denote as μ_0 and μ_1 the merit figures of the main band, peaked at 640 nm, and of the vibronic band, peaked at 590 nm, respectively. For a given wavelength λ, the dye molecule has a probability $p_0(\lambda)$ of being excited in the main band and $p_1(\lambda)$ of being excited in the vibronic band. We assumed for p_0 and p_1 a typical Gaussian +Lorentzian shape, and determined all the corresponding distribution parameters by means of a fit to the absorption spectrum. If the dye excitations in either of the two bands can be considered as independent statistical processes, the effective merit figure is given by

$$\mu(\lambda)=\frac{p_0(\lambda)\mu_0+p_1(\lambda)\mu_1}{p_0(\lambda)+p_1(\lambda)}. \tag{12}$$

We used this expression to fit the observed wavelength dependence of μ, by adjusting the two parameters μ_0 and μ_1. The best-fit outcome, corresponding to $\mu_0=2200$ and $\mu_1=1300$, is shown in Fig. 4 as a solid line.

In AD1, the involved vibration optical mode should consist mainly of a stretch of the substituent groups NH_2 and OH. The excitation of this internal vibration lowers the molecule overall reorienting efficiency. This is a further indication of the major role played by the interactions between the substituent polar groups and the host. A similar decrease of efficiency for higher photon energy (lower wavelengths) has been reported in Ref. 12. We suggest three possible explanations. First, if the vibrational state is sufficiently long-lived, the vibration could effectively reduce the intermolecular polar interactions of the substituent groups with the host. Second, the vibronic state could have more decay channels than the main electronic state, leading to a shorter lifetime, or to trapping into ineffective triplet states, or to photochemical transformations, all effects reducing the reorienting efficiency. Third, as proposed in Ref. 12, the vibrational relaxation immediately following the photon absorption, although very fast, could release enough energy to reorient randomly the excited dye molecule, again reducing its average aligning effect.

V. COMPARISON WITH THEORY

We now try a more quantitative analysis of our experimental results in terms of the kinetic molecular model reported in Ref. 19. Let us first briefly recall here the basic assumptions and notations of the model.

A. Molecular model

Consider a linearly polarized light wave passing through an absorbing nematic LC obtained by dissolving a small amount of dichroic dye in a transparent host. We suppose that the dye molecules behave as rod-like molecules with a molecular axis specified by a unit vector $\boldsymbol{s}$, or by its polar angles θ and ϕ with respect to a z axis oriented as the molecular director $\boldsymbol{n}$. For the dye excitation we make a two level approximation, and label with the subscripts g and e the ground and excited state, respectively. The numbers of ground-state and excited dye molecules per unit volume and solid angle at time t and orientation $\boldsymbol{s}$ are denoted as $f_g(\boldsymbol{s},t)$ and $f_e(\boldsymbol{s},t)$. The total number N_d of dye molecules per unit volume is assumed small with respect to the host number density.

The rotational dynamics of dye molecules is ruled by intermolecular interactions with the LC host. The equilibrium interactions are described within a mean-field approximation. Following Jánossy's idea, the mean-fields for excited and ground-state molecules are allowed to be different. We take them in the following form:

$$U_\alpha(\theta)=-\tfrac{1}{2}u_\alpha S\cos^2\theta \quad (\alpha=g,e), \tag{13}$$

where S is the LC host order parameter and u_e and u_g are material coefficients measuring the dye-host orientational interaction strength (note the change of notations with respect to Ref. 19). Nonequilibrium kinetic interactions between dye and LC host are modeled by the molecule rotational friction coefficients η_g and η_e, or equivalently by the rotational diffusion constants $D_g=kT/\eta_g$ and $D_e=kT/\eta_e$.[40,41]

When the light intensity is zero, the excited-state population is empty, i.e., $f_e=0$, and the ground-state orientational distribution reduces to the equilibrium Boltzmann one

$$f_d=N_d\frac{e^{-\frac{U_g}{kT}}}{\int e^{-\frac{U_g}{kT}}\,d\Omega}. \tag{14}$$

The effect of light absorption is to introduce a probability per unit time $p(\boldsymbol{s})$ for a ground-state dye molecule to get excited. If the dye electronic transition dipole forms an angle ψ with the molecule long axis $\boldsymbol{s}$, then

$$p(\boldsymbol{s})=\sigma|E|^2[\tfrac{1}{3}(1-A)+A(\boldsymbol{e}\cdot\boldsymbol{s})^2], \tag{15}$$

where σ is a constant proportional to the absorption cross section (including also local-field factors) and $A=(3\cos^2\psi-1)/2$. In particular $A=1$ for molecules having their transition dipole parallel to $\boldsymbol{s}$. The molecular constants σ and A can be related to the absorption coefficients by equating the power lost by the light wave to the photon energy $h\nu$ times the number of dye excitations induced per unit time. We obtain

$$\sigma N_d=\frac{c(n_e\alpha_e+2n_o\alpha_o)}{8\pi h\nu} \tag{16}$$

and

$$AS_g=\frac{n_e\alpha_e-n_o\alpha_o}{n_e\alpha_e+2n_o\alpha_o}, \tag{17}$$

where S_g is the ground-state dye order parameter

$$S_g=\langle(3\cos^2\theta-1)/2\rangle_d=\frac{1}{N_d}\int d\Omega\ \frac{3\cos^2\theta-1}{2}f_d. \tag{18}$$

Equation (17) is used to calculate S_g from the measured dichroism (the absolute value of A must be known independently).

The kinetic equations are given by the following set of Einstein–Smoluchowsky diffusion equations for the rotational diffusion of the two dye populations, coupled by the photoinduced transitions:

$$\frac{\partial f_\alpha}{\partial t} - D_\alpha \overline{\nabla^2} f_\alpha - \frac{D_\alpha}{kT} \overline{\nabla} \cdot [f_\alpha \overline{\nabla} U_\alpha]$$

$$= (\pm)_\alpha \left[p f_g - \frac{f_e}{\tau_f} \right], \quad \alpha = g, e, \tag{19}$$

where $\overline{\nabla}$ is the angular part of the ordinary ∇ differential operator, τ_f is the excited-state lifetime, and $(\pm)_\alpha$ is $+$ for $\alpha = e$ and $-$ for $\alpha = g$.

After solving Eq. (19) for the steady-state distributions f_e and f_g, or equivalently for the deviations from equilibrium $f'_e = f_e, f'_g = f_g - f_d$, the photoinduced torque can be obtained as the total mean-field torque exchanged between dye and nematic host, i.e.,

$$\boldsymbol{\tau}_{\mathrm{ph}} = \int d\Omega \;\; \mathbf{s} \times (f_e \overline{\nabla} U_e + f_g \overline{\nabla} U_g)$$

$$= \int d\Omega \;\; \mathbf{s} (f'_e \overline{\nabla} U_e + f'_g \overline{\nabla} U_g). \tag{20}$$

Equation (19) cannot be solved analytically. An approximate and/or numerical approach is needed. It is convenient passing to dimensionless quantities. For brevity we do not report the intermediate steps explicitly. It is however important to point out that the resulting dimensionless equations depend only on the following four dimensionless parameters: (i) The normalized ground-state energy $m_g = u_g S/2kT$, that is in one-to-one correspondence with the dye order parameter S_g, as specified by Eqs. (14) and (18); (ii) the mean-field energy ratio u_e/u_g; (iii) the friction coefficient (or diffusion constant) ratio $\eta_e/\eta_g = D_g/D_e$; (iv) the reduced lifetime $\tau_f D_e$. The merit figure μ can be shown to be given by $\mu = (AkT)/(hD_eS) \cdot \tilde{\mu}(m_g, u_e/u_g, D_g/D_e, \tau_f D_e)$, where $\tilde{\mu}$ is function only of the above mentioned 4 dimensionless parameters.

To solve numerically the steady-state dimensionless equations corresponding to Eqs. (19), we projected them onto the $Y_{l,m}(\theta, \phi)$ spherical harmonic basis, thus obtaining an infinite set of coupled algebraic equations. This set was solved by considering only the spherical components having $l \leqslant l_{\max}$, where $l_{\max}$ was increased automatically until stability was achieved (typically $l_{\max} \sim 10-20$). Some examples of our results are plotted in Fig. 5. The actual value of μ depends on the exact value of the scaling factor $AkT/100hD_eS$, which is of the order of 1000. Our results are consistent with those already reported in Ref. 18, where only the case $D_g/D_e = 1$ was considered.

It is seen from Fig. 5 that in the region $u_g S/2kT < 2$ the lines are approximately straight, i.e., the torque is proportional to $u_g S$. This limit can be also calculated analytically, as reported in Ref. 19. In our notations, we have

$$\mu \simeq \frac{2A}{15h} \frac{\tau_f D_e}{1 + 6 D_e \tau_f} \left(\frac{u_e}{D_e} - \frac{u_g}{D_g} \right). \tag{21}$$

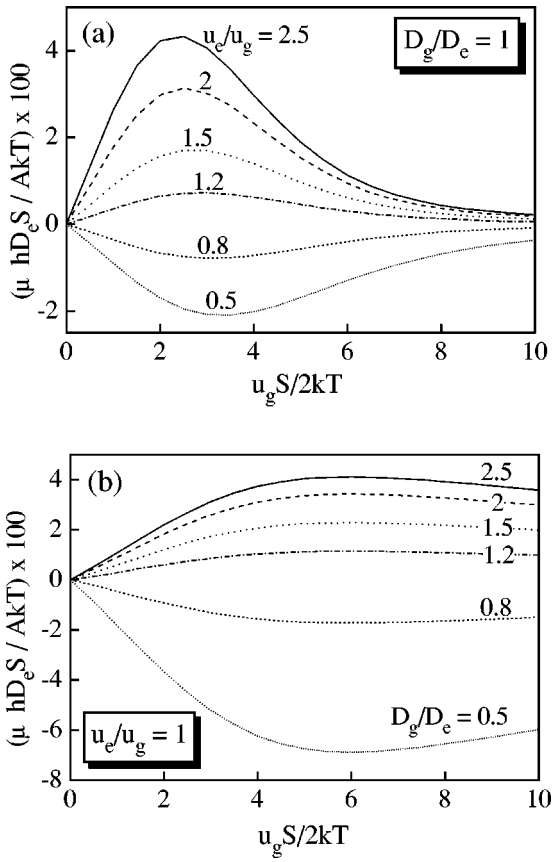

FIG. 5. Theoretical merit figure μ times the material-dependent scale factor $100hD_eS/AkT$ vs ground-state guest–host interaction parameter $m_g = u_g S/2kT$ for different effects of electronic excitation on intermolecular interaction parameters. In (a) we set $D_g/D_e = 1$ and varied the energy ratio u_e/u_g. In (b) we set $u_e/u_g = 1$ and varied the ratio D_g/D_e. In all plots we set $D_e \tau_f = 0.1$, close to the value measured for AD1 in E63.

This expression of μ remains valid even in the isotropic phase.[15]

Consider now the opposite limit of large $m_g = u_g S/2kT$. As shown in Fig. 5(a), in this limit μ vanishes very fast if $D_e = D_g$. Even a very large ratio u_e/u_g cannot give significant values of μ, in the range $m_g > 6$. On the contrary, the effect of the diffusion constant ratio D_g/D_e does not vanish, as shown in Fig. 5(b). This behavior can be understood by inspection of Eq. (19). Indeed, if m_g is large, the energy terms U_α dominate against the diffusive term in the left-hand side of Eq. (19). In this case, at steady state, the approximate relationship $f'_e/f'_g \sim -u_g D_g/u_e D_e$ holds true, and the photoinduced torque given by Eq. (20) vanishes if $D_e = D_g$. Therefore, if a mixture has $m_g > 6$ corresponding to a dye order parameter $S_g > 0.7$ (as in AD1-E63 at room temperature), the photoinduced torque is essentially determined by the change in diffusion constants and not by the change in equilibrium mean-fields. However, we cannot exclude that this rather drastic result of our model be a consequence of the single-Legendre-mode angle dependence assumed for the mean-field potentials, in Eq. (13).

TABLE III. Calculated parameters of dye-LC mixture corresponding to measured merit figures.

Dye-LC	u_e/u_g $(D_g=D_e)$	D_g/D_e $(u_e=u_g)$	$u_e/u_g=$ D_g/D_e
AD1-5CB	2.7	1.95	1.39
AD1-E63	>10	1.80	1.55
AD1-MBBA	1.21	1.23	1.10
AD2-5CB	1.10	1.05	1.03
AD2-E63	1.47	1.04	1.04
AD2-MBBA	$\simeq 1$	$\simeq 1$	$\simeq 1$
AD3-5CB	0.83	0.87	0.92
AD3-E63	0.88	0.91	0.95
AD3-MBBA	0.85	0.88	0.93

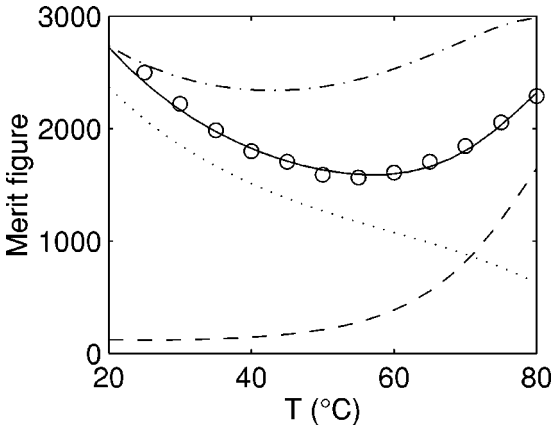

FIG. 6. Experimental and theoretical temperature behavior of merit figure μ for a mixture of AD1 in E63. Data are from Ref. 6. Solid line is a best-fit obtained as described in the text. Dashed line corresponds to assuming $D_e=D_g$ and the same u_e/u_g as in solid line. Dotted line to assuming $u_e=u_g$ and the same D_g/D_e as in solid line. Dot–dash line is for $u_e=u_g$ and a temperature independent D_g/D_e.

B. Data analysis

In the case of AD1 in E63 we know the values of D_e and τ_f from Ref. 42. Therefore, we may interpret the merit figure data quantitatively using our model. For comparison, we also extended such calculations to the other mixtures, by assuming that the values of D_e and τ_f are the same. This is probably a reasonable approximation for AD1 in 5CB and (less) in MBBA, but it is not good for mixtures with other dyes; therefore the results for AD2 and AD3 cannot be considered realistic.

In all mixtures, the value of u_g is deduced from the measured dichroism, using first Eq. (17) to determine the dye order parameter and next Eq. (18) to determine the factor $u_gS/2kT$ (S is in Table I). The change in intermolecular forces is modeled with the two unknown parameters u_e/u_g and $\eta_e/\eta_g=D_g/D_e$. For each mixture we have only one input piece of data, i.e., the merit figure μ, so that these two parameters cannot be determined without further assumptions. Tentatively, we may try to set either $D_g=D_e$ or $u_e=u_g$. The corresponding results are reported in Table III. It is seen that the hypothesis $D_g=D_e$ leads to values of u_e/u_g that are too large to be realistic in several cases. This is due to the rapid vanishing of μ for large values of $m_g=u_gS/2kT$, as shown in Fig. 5(a). On the contrary, it is quite possible that $u_e\simeq u_g$ and that the effect is mainly caused by the variation of diffusion constants. The intermediate case $u_e/u_g=D_g/D_e$ was also considered and reported in Table III. It is noteworthy that the lower merit figure of the mixtures with E63 host compared to 5CB does not correspond to equally lower changes in diffusion constants or interaction energies. The reason why E63 is less effective than 5CB is related instead to the higher order parameter S in E63.

We point out that a large change of the rotational friction coefficient requires only a relatively small change in the intermolecular forces. An *ab initio* statistical theory of the friction coefficient is reported in Ref. 41. Although the model is based on pure van der Waals intermolecular interactions, its main qualitative results are likely to be generally valid. According to it, the expression of the diffusion constant can be cast in the following Arrhenius-type form

$$D=D_0e^{-\frac{E_0+E_1}{kT}}, \tag{22}$$

where the preexponential factor is given by $D_0=CE_0^3T^{-4.5}$, C being a constant independent of temperature and interaction energies, E_0 is an energy characterizing the isotropic attraction between the dye molecule and the neighbors, and E_1 is an energy contributing to the orientational mean-field interaction u_α. For organic molecules such as those considered in this work, at room temperature, $E_0/kT\sim 10$ or more, while $E_1/kT\sim 1$. Therefore a very small relative change in E_0 may lead to a strong relative variation of D. For example, a fractional change of only 10% in E_0 would correspond to a change of D roughly by a factor 2.

C. Temperature dependence

The temperature behavior of μ is to a good approximation the same as that of the enhancement ratio $\eta=\zeta/\epsilon_a$. This can be seen from Eq. (2), from the fact that ϵ_a and S have approximately the same temperature dependence, and that the isotropic combination $n_e\alpha_e+2n_o\alpha_o$ is weakly dependent on temperature. From the data published in Ref. 6 on $\eta(T)$, we calculated a set of points for $\mu(T)$ in the AD1-E63 mixture, reported in Fig. 6 as circles.

The best-fit on the data based on our model is shown as a solid line in the same figure. The host order parameter versus temperature $S(T)$ was obtained from magnetic anisotropy data.[25] For the diffusion constants D_e and D_g we assumed the Arrhenius-like temperature behavior given by Eq. (22). The temperature dependence of D_e and τ_f was also measured, as reported in Ref. 42. From a fit based on Eq. (22) of the measured $D_e(T)$, we obtained the excited-state activation energy $E_{0e}+E_{1e}=22$ kJ/mol. The value of $u_g=60$ kJ/mol was obtained from the measured dichroism, as described previously. The remaining unknown parameters were adjusted to fit the observed $\mu(T)$. They were (i) the activation energy difference $\Delta E=(E_{0e}+E_{1e})-(E_{0g}+E_{1g})$ for excited and ground states of the dye; (ii) the (temperature independent) ratio of the preexponential factors D_{0g}/D_{0e}; (iii) the ratio of the orientational energies u_e/u_g, assumed to

be temperature independent. The best-fit results were (i) $\Delta E = 4.5$ kJ/mol, (ii) $D_{0g}/D_{0e} = 0.22$, (iii) $u_e/u_g = 1.33$. These values correspond to a diffusion constant ratio $D_g/D_e = 1.4$ at $T = 20°C$ and $D_g/D_e = 1.1$ close to the clearing temperature. Note that the activation energy relative change $\Delta E/E$ is a reasonable 20%. The variation ΔE is larger but of the same order as that resulting from the solvent shift in the absorption spectrum. Moreover, it is in the range of the hydrogen–bond strength variations directly observed in other experiments.[33,35,36] If the dependence of the preexponential factors on E_0 is assumed to be $D_0 \propto E_0^3$, as suggested in Ref. 41, then we also obtain $E_{0g}/E_{0e} \approx 0.6$.

We also tried to fit the data with less adjustable parameters, assuming first $D_g/D_e = 1$ and next $u_e/u_g = 1$. In the first case, there is no way to fit the data for a finite ratio u_e/u_g. The theoretical curve $\mu(T)$ obtained setting $D_g/D_e = 1$ and $u_e/u_g = 1.33$ is reported in Fig. 6 for comparison, as a dashed line. In the second case, where D_g/D_e is varied and $u_e/u_g = 1$, we could not fit the data using the activation temperature dependence only, or assuming a temperature-independent ratio D_g/D_e. It is however possible to fit the data by assuming a nonmonotone temperature behavior of D_g/D_e. For comparison, with the dotted line in Fig. 6 is reported the theoretical value of $\mu(T)$ for $u_e/u_g = 1$ and $D_g(T)/D_e(T)$ as in the best-fit case reported above. The dot–dash line corresponds to $D_g/D_e = 1.65$, temperature independent. In the last case, although a nonmonotone behavior is correctly predicted, it is too weak to explain the data, and this remains true for any temperature independent value of the ratio D_g/D_e.

VI. CONCLUSIONS

We have observed that the phenomenon of photoinduced molecular reorientation of dyed nematic liquid crystals depends dramatically on the specific intermolecular forces exchanged between dye and host. For some dyes, hosts capable of polar interactions enhance the effect by a large factor, showing that dipole–dipole or hydrogen–bond forces can be important. The most effective of these dyes shows also a significant solvent-induced shift, consistent with the hypothesis that polar interactions are enhanced in excited dye molecules. This hypothesis is also supported by molecular orbital calculations that predict a significant intramolecular charge transfer in the electronic transition. These results are in favor of Jánossy's interpretation of the reorientation effect as resulting from a photoinduced change of intermolecular forces in excited dye molecules.

According to Jánossy's original idea, the force variation is reflected essentially in a change of the mean-field for dye orientation in the nematic host. However, to obtain a quantitative agreement between the experimental results and a molecular kinetic model, we were obliged to assume also a variation of the molecular rotation friction coefficient or diffusion constant in excited dye molecules. Actually, an *ab initio* molecular model predicts the rotational friction coefficient to be a sensitive function of intermolecular forces, making our assumption quite plausible. In our view, large photoinduced changes of molecular physical parameters can occur even with no conformational transformations. Most anthraquinone derivatives are known not to undergo conformational photo-transformations. Conformation changes are probably important for other classes of dyes (as azo-dyes) which induce negative reorientation (i.e., away from the electric field) and show no significant sensitivity to the host structure. We are currently planning an experiment for measuring the kinetic molecular parameters of dyes in solutions, both in the ground and excited state. The outcome of such experiment will probably provide a final test for our understanding of the photoinduced liquid crystal reorientation effect.

ACKNOWLEDGMENTS

We are indebted to M. Colicchio for helping in the absorption spectra measurements, to M. Ricci (LENS) for the fluorescence spectra, and to G. Abbate for useful discussions. This work was supported by MURST (Ministero dell'Università e della Ricerca Scientifica e Tecnologica) and INFM (Istituto Nazionale Fisica della Materia).

[1] A. S. Zolot'ko, V. F. Kitaeva, N. Kroo, N. I. Sobolev, and L. Csillag, Pis'ma Zh. Eksp. Teor. Fiz. **32**, 170 (1980).
[2] S. D. Durbin, S. M. Arakelian, and Y. R. Shen, Phys. Rev. Lett. **47**, 1411 (1981).
[3] For a review see, e.g., N. V. Tabiryan, A. V. Sukhov, and B. Ya. Zel'dovich, Mol. Cryst. Liq. Cryst. **136**, 1 (1986); L. Marrucci and Y. R. Shen, in *The Optics of Thermotropic Liquid Crystals*, edited by R. Sambles and S. Elston (Taylor and Francis, London, 1997).
[4] I. Jánossy and a. D. Lloyd, and B. S. Wherrett, Mol. Cryst. Liq. Cryst. **179**, 1 (1990).
[5] I. Jánossy and A. D. Lloyd, Mol. Cryst. Liq. Cryst. **203**, 77 (1991).
[6] I. Jánossy, L. Csillag, and A. D. Lloydl, Phys. Rev. A **44**, 8410 (1991).
[7] I. Jánossy and T. Kósa, Opt. Lett. **17**, 1183 (1992).
[8] I. C. Khoo, H. Li, and Y. Liang, IEEE J. Quantum Electron. **29**, 1444 (1993).
[9] D. Paparo, P. Maddalena, G. Abbate, E. Santamato, and I. Jánossy, Mol. Cryst. Liq. Cryst. **251**, 73 (1994).
[10] A. S. Zolot'ko, V. F. Kitaeva, and D. B. Terskov, Jr. Zh. Eksp. Teor. Fiz. **106**, 1722 (1994).[Sov. Phys. JETP **79**, 931 (1994)].
[11] M. I. Barnik, A. S. Zolot'ko, V. G. Rumyantsev, and D. B. Terskov,Kristallografiya **40**, 746 (1995). [Sov. Phys. Crystallogr. **40**, 691 (1995)].
[12] T. Kósa and I. Jánossy, Opt. Lett. **20**, 1230 (1995).
[13] L. M. Blinov, M. I. Barnik, A. Mazzulla, and C. Umeton, Mol. Mater. **5**, 237 (1995).
[14] L. M. Blinov, J. Nonlinear Opt. Phys. Mater. **5**, 165 (1996).
[15] D. Paparo, L. Marrucci, G. Abbate, E. Santamato, M. Kreuzer, P. Lehnert, and T. Vogeler, Phys. Rev. Lett. **78**, 38 (1997).
[16] R. Muenster, M. Jorasch, X. Zhuang, and Y. R. Shen, Phys. Rev. Lett. **78**, 42 (1997).
[17] S. P. Palto and G. Durand, J. Phys. (France) **5**, 963 (1995).
[18] I. Jánossy, Phys. Rev. E **49**, 2957 (1994).
[19] L. Marrucci and D. Paparo, Phys. Rev. E **56**, 1765 (1997).
[20] I. C. Khoo, T. H. Liu, and P. Y. Yan, J. Opt. Soc. Am. B **4**, 115 (1987).
[21] M. Tamburrini, E. Ciaramella, and E. Santamato, Mol. Cryst. Liq. Cryst. **241**, 205 (1994).
[22] Details about dichroic dyes designed for mixing in liquid crystals and their preparation can be found in Refs. 23 and 24.
[23] N. Basturk, J. Cognard, and T. Hieu Phan, Mol. Cryst. Liq. Cryst. **95**, 71 (1983).
[24] A. V. Ivashchenko, *Dichroic Dyes for Liquid Crystal Displays* (CRC, Boca Raton, Florida, 1994).

[25] A. Jákli, D. R. Kim, M. R. Kuzma, and A. Saupe, Mol. Cryst. Liq. Cryst. **198**, 331 (1991).
[26] J. Israelachvili, *Intermolecular & Surface Forces* (Academic, London, 1985).
[27] S. Imazeki, A. Mukoh, N. Tanaka, and M. Kinoshita, Mol. Cryst. Liq. Cryst. **225**, 197 (1993).
[28] E. A. Power and T. Thirunamachandran, Phys. Rev. A **51**, 3660 (1995).
[29] H. Inoue, T. Hoshi, J. Yoshino, and Y. Tanizaki, Bull. Chem. Soc. Jpn. **45**, 1018 (1972).
[30] J. D. Petke, P. Butler, and G. M. Maggiora, Int. J. Quantum Chem. **27**, 71 (1985).
[31] B. O. Myrvold, J. Spanget-Larsen, and E. W. Thulstrup, Chem. Phys. **104**, 305 (1986).
[32] Marilena Ricci, LENS Firenze (private communication).
[33] S. Suzuki and H. Baba, J. Chem. Phys. **38**, 349 (1963).
[34] S. Nagase and T. Fueno, Theor. Chim. Acta **35**, 217 (1974).
[35] H. Abe, N. Mikami, M. Ito, and Y. Udagawa, J. Phys. Chem. **86**, 2567 (1982).
[36] A. G. Taylor, A. C. Jones, and D. Phillips, Chem. Phys. Lett. **169**, 17 (1990).
[37] J. Zeng, N. S. Hush, and J. R. Reimers, J. Chem. Phys. **99**, 1496 (1993).
[38] V. Barone, G. Milano, L. Orlandini, and C. Adamo, J. Chem. Soc. Perkin Trans. 2, 1141 (1995).
[39] N. G. Bakhshiev, O. P. Girin, and I. V. Piterskaya, Opt. Spektrosk. **24**, 901 (1968) [Opt. Spektrosk. **24**, 483 (1968)].
[40] M. Doi and S. F. Edwards, *The Theory of Polymer Dynamics* (Oxford University Press, Oxford, 1986).
[41] M. A. Osipov and E. M. Terentjev, Z. Naturforsch. Teil A **44**, 785 (1989).
[42] D. Paparo, L. Marrucci, G. Abbate, E. Santamato, P. Bartolini, and R. Torre, Mol. Cryst. Liq. Cryst. **282**, 461 (1996).